

Control of a spacecraft using a reaction control system

John D. Foley
Martin Marietta Space Systems
P.O. Box 179
Denver, Colorado 80201

ABSTRACT

This paper describes the design and simulation of a spacecraft pointing control system used to track a moving target using only a Reaction Control System (RCS) for generation of control torques. In this system the target is moving but the target angular position and rate cannot be directly measured. A tracking sensor generates only an angular error to the control loop.

In order to reduce cost and increase reliability, the thrusters are operated in a bang-bang mode. As a result there is a steady state limit cycle after the error has been reduced to a minimum level. A digital control algorithm has been developed that is based on angular error between the target and pointing angles, and derived angular error rate. This algorithm drives the error to a minimum in the shortest time possible given the limited thrust available from the RCS thrusters.

The simulation shows that the steady state error can be made surprisingly small if two or more torque levels are used. The error is dictated primarily by the width of the dead band as set by the control logic. The effect of the noise in the error signal is simulated as well as the time delay and hysteresis in the thrusters. The simulation also shows that the rate of fuel consumption and the frequency of the limit cycle are very low.

INTRODUCTION

The simulation program is split up into six blocks of code: an initial section where all constants are initialized, a continuous section, a discrete section for the RCS controller, a discrete section to handle the torque delays, and two discrete sections to handle any external disturbances (such as a scanning mirror). Integrations to obtain angle and angle rate take place in the continuous section. The torque level is also chosen in this section. The RCS discrete section contains code which generates the error (including noise), the derived rate, the switching line, and the torque magnitude. It also selects

positive, negative, or zero torque (reaction jet firings) depending on whether or not the error is within one deadband of the switching line. This section also handles the delay using the Schedule operator. This operator makes it possible to set a delay on the selected torque. The turn-on delay and the turn-off delay can be set independently.

Each of the above features is implemented in the simulation, which is written using Advanced Continuous Simulation Language (ACSL).

PHASE PLANE LOGIC

Given a maximum torque level, an angle rate, and an initial angle, the simulation calculates a new angle (switching line). This switching line is used to turn the reaction jets on and off. To obtain a relationship for the switching line, one starts with $T = J \ddot{\theta}$ (where T is torque and J is rotational inertia) or,

$$\ddot{\theta} = \frac{T}{J} . \quad (1)$$

One integration of this equation yields:

$$\dot{\theta} = \frac{T}{J} t + \dot{\theta}_0 \quad (2)$$

and integrating again, assuming zero initial angle rate, gives:

$$\theta = \frac{T}{2J} t^2 + \theta_0 . \quad (3)$$

Solving equation (2) for the minimum time trajectory for θ versus $\dot{\theta}$,

$$t_{\min} = \frac{\dot{\theta} J}{T_{\max}} \quad (4)$$

and substituting the result from (4) back into equation (3), a general equation relating the past angle and angle rate with the present angle is obtained:

$$\theta = \frac{\dot{\theta}^2 J}{2T} + \theta_0 . \quad (5)$$

Equation (5) describes the parabola opening to the right in Figure 1. However, for the purposes of the simulation, the switching line must have the shape of solid line #1 in Figure 1, which is comprised of parts of two parabolas. Therefore, the equation for the switching line must be altered to meet the requirements.

$$\dot{\theta} = -\frac{\dot{\theta}|J}{2T} + \theta_0 \quad (6)$$

Equation (6) is now the correct equation for the switching line. The trajectory of angle versus angle rate will follow the shape of one of the solid curves depending on which torque level is chosen. If a high torque magnitude is chosen, then a large angle rate will result, as in switching line #1. A large torque will be used in the case of large reorientations of the spacecraft in order to minimize time required to slew. Likewise, if a low torque magnitude is chosen, the trajectory follows switching line #2. Lower torque is used for fine tracking of a target in order to keep angular rates small and firings of the reaction jets to a minimum. This technique minimizes fuel consumption since the majority of time is spent in fine tracking mode.

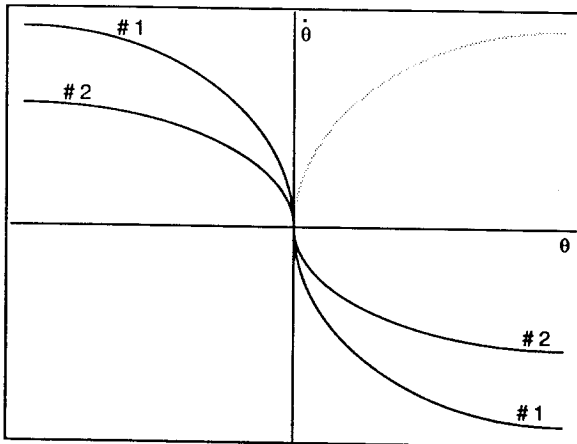


Figure 1. Phase plane switching lines

A closer examination of the switching line mechanics reveals how a deadband and hysteresis may be included in the simulation. To conserve fuel, there is a region on either side of the switching line where no thrust is applied. This drift region or deadband dictates the pointing accuracy of the spacecraft. Figure 2 is a blowup of a section of the switching line in the upper left quadrant of Figure 1. As Figure 2 illustrates, starting at Point 1, positive torque is applied to reduce the error; and as a result, the angle rate increases. This is continued until the deadband, Point 2, is reached, where the jets are turned off.

The spacecraft drifts through this region with a constant angular rate, while the angle error is continuing to decrease. When the other side of the deadband is reached, Point 3, the jets are turned back on but in the opposite direction to slow down the spacecraft while continuing to reduce the angular error. Ten percent hysteresis is added to the control system to prevent thruster valve chatter. This chatter would be a problem at low spacecraft angular rates and high sensor noise levels. Therefore, the jets are turned off slightly after the deadband is reached at Point 2, and turned back on slightly after the deadband is exited at Point 3.

The results of a typical simulation run are shown in the phase plane plot of Figure 3. The spacecraft is required to track an accelerating

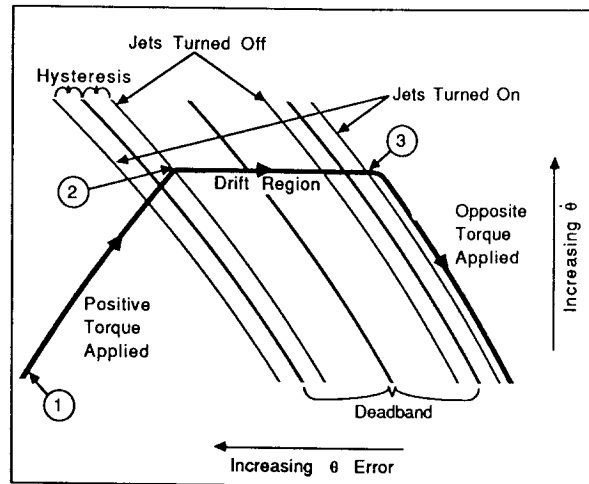


Figure 2. Details of phase plane switching lines

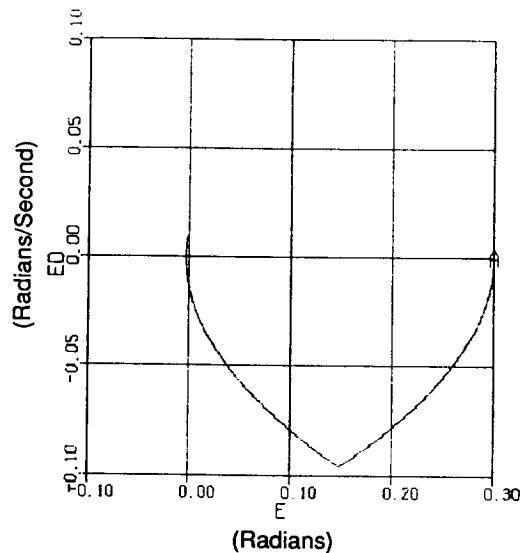


Figure 3. Phase plane response with an initial error of 0.3 radians

target with an initial error of 0.3 radians. Maximum torque is applied to reduce the angle error until the switching line is encountered. Once the deadband is passed, the torque is reversed.

In Figure 4, the effect of two different torque levels can be seen. When the angle error and angle rate become sufficiently small, the torque level is reduced and a different switching line curve is followed. This is coincident with curves like those shown in Figure 1.

Ideally, this switching line would result in zero angle error and zero angle rate at the same

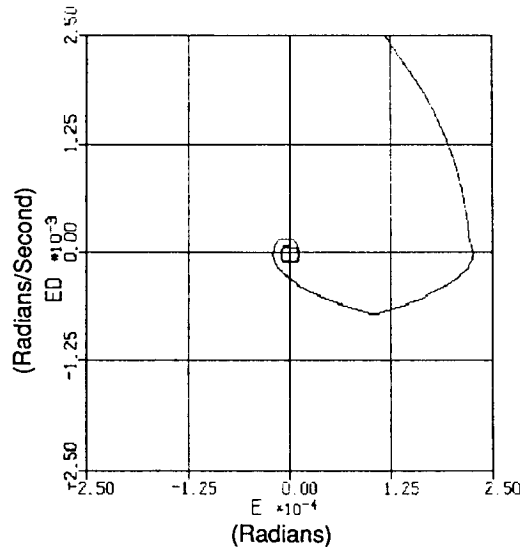


Figure 4. Phase plane response showing the effect of changing torque levels

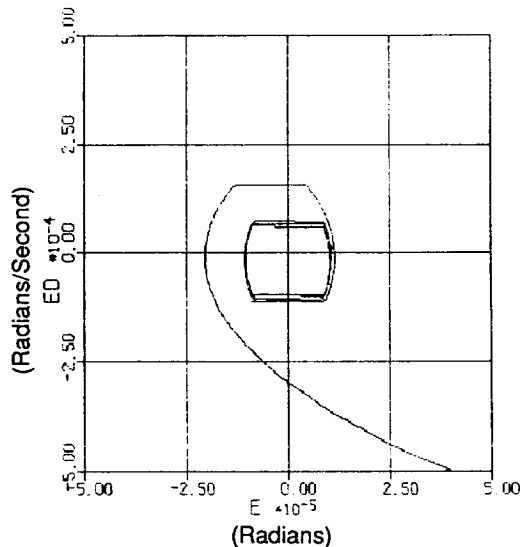


Figure 5a. Expanded phase plane plot showing the limit cycle

instant. This would be true if there were zero deadband and no hysteresis. Since this is not the case in a real system, a limit cycle is reached when the error is small (the size of the deadband). From the shape of the switching lines in Figure 1, one can see that the parabolic trajectory will be followed, crossing the zero angular rate line and continuing around until the other part of the switching line is reached. The process keeps repeating, creating a limit cycle about the origin of the phase plane as shown in figure 5a which is an expansion of Figure 4. The limit cycle represents the spacecraft's oscillation about zero angle error. In the time domain, the error stays within the limits of the deadband, as shown in Figure 5b.

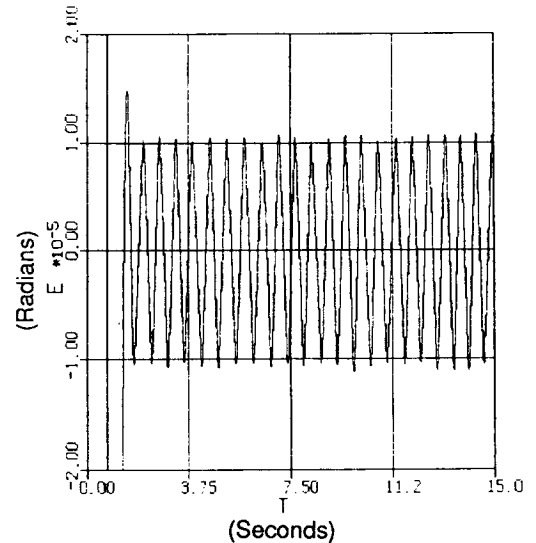


Figure 5b. Time response of angle error

TIME DELAYS DUE TO THRUSTER MECHANISM

There are delays in turning on and off the thrusters, which are due to the electromechanical valve systems on the reaction control jets. If there were no delays, the torque profile would be a square wave, shown in Figure 6a, corresponding to instantaneous turn-on and turn-off. However, in a real valve system, the torque profile is smoothed with finite rise and fall times, as is shown in Figure 6b. For the simulation, this non-linear profile can be approximated by a square wave which contains an equal amount of torque area under its profile. This effect is shown in Figure 6c.

EFFECTS OF AN EXTERNAL DISTURBANCE

A disturbance to the spacecraft, such as that created by a scanning mirror, may be included in the simulation by adding a torque of the correct magnitude and time response to the torque

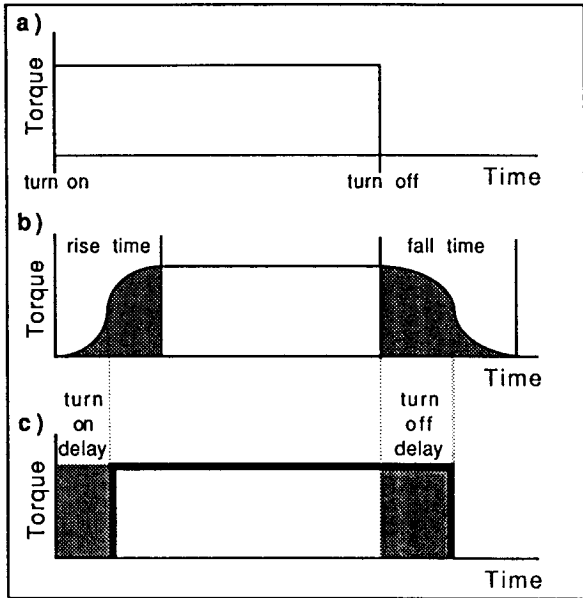


Figure 6. a) Ideal torque profile b) Actual torque profile c) Simulated torque profile

generated by the thrusters. In the case of a scanning mirror, a sinusoidal torque (seen in Figure 7) with magnitude in accordance with the inertia of the mirror simulates accurately the dynamics of the mirror moving back and forth against soft stops. The maximum torque would be at the extremes of its range of motion. The limit cycle of the RCS is shown in Figure 8. The time response shows, when compared with that of the case with no external disturbance (Figure 6), that with the disturbance the limit cycle extends farther outside the deadband of 10 microradians. This means the thrusters will be on for longer

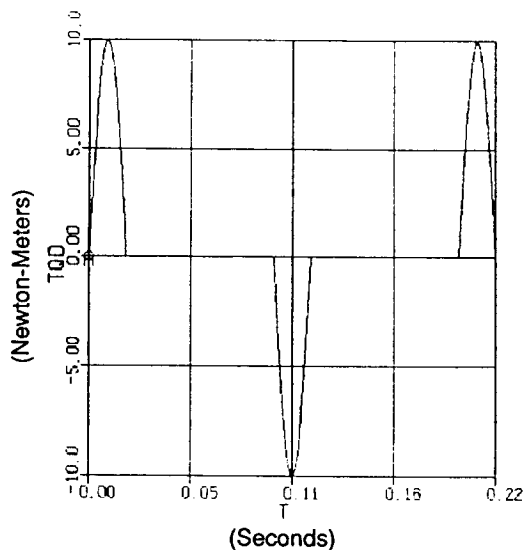


Figure 7. Scanning mirror disturbance torque

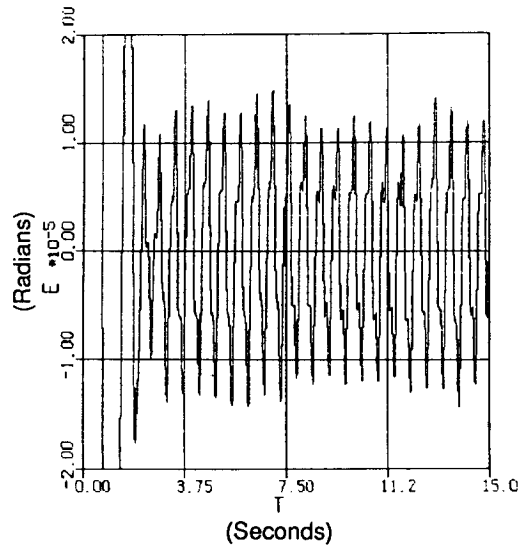


Figure 8. Time response of angle error including disturbance torques

periods of time in order to force the error back to within the deadband. Hence, more fuel is used. For the torque levels simulated and shown here, there was about a 3.6 to 1 ratio in fuel consumption for the case with a disturbance during the limit cycle over the case with no disturbance.

PARAMETRIC STUDIES

The simulation code contains an external file which allows one to make successive runs with different values for certain constants without recompiling the main code. This makes it possible to perform parametric studies on the physical variables of the spacecraft.

In Figures 9 and 10, inertia ranges from 1000 to 4000 kg-m². Figure 9 shows that settling time increases linearly with increasing inertia; in this case, settling time refers to the time it takes for

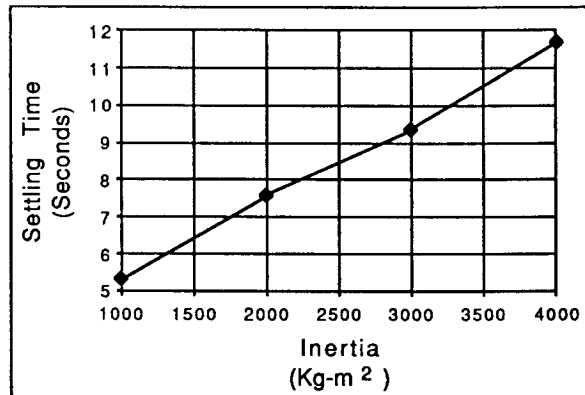


Figure 9. Settling time as a function of spacecraft's inertia

the error to reach and remain within the limit cycle amplitude. The linear relationship of fuel consumption to inertia is shown in Figure 10.

As was previously stated, the width of the deadband dictates the pointing accuracy of the spacecraft. However, one must trade off optimized fuel consumption for higher pointing accuracy. Figure 11 exhibits the increase in fuel consumption with higher desired pointing accuracy. Half deadband width is shown on the plot since that is the form of the variable used in the simulation.

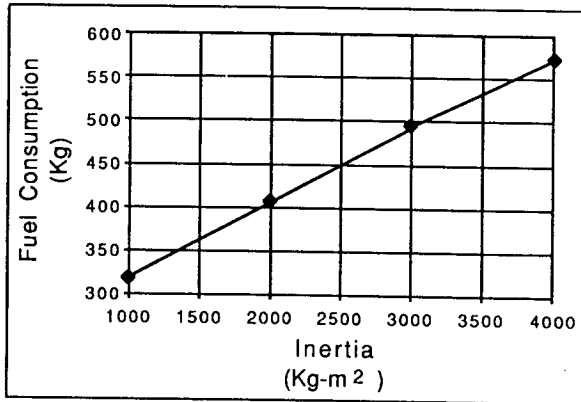


Figure 10. Fuel consumption as a function of spacecraft's inertia

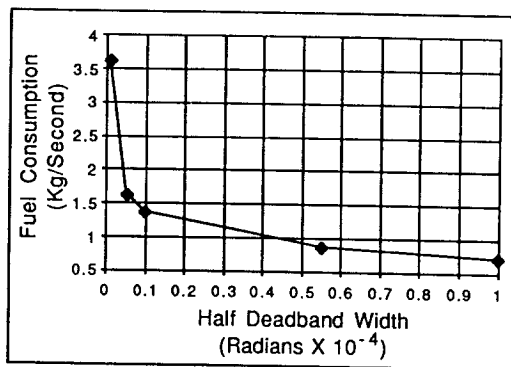


Figure 11. Fuel consumption as a function of deadband width

SUMMARY

In this paper, a model describing the dynamics of a Reaction Control System has been presented. Effects such as time delays, hysteresis, and external disturbances to the spacecraft, among others, have been incorporated into the simulation. The flexibility of the simulation (written in ACSL) allows one to perform many types of parametric studies, of which only a few have been discussed here.

Perhaps the most important discovery from the simulation is that the width of the deadband completely dictates the pointing accuracy of the spacecraft. Of course, higher pointing accuracy requirements increase the amount of fuel consumed since there will be more thruster firings for a smaller deadband.